Refractive index reconstruction of a zinc oxide thin film electrodeposited on glass substrates applied in a GaAs PIN photodiode

T. Mouet [a,b,*], A. Saouli [b], A. Mouatsi [a], B. Kaghouche [c,d], L. Dib [c,e], I. Nouicer [f]
[a] *Faculty of Process Engineering, Salah Boubnider University of Constantine 3, Constantine, Algeria*
[b] *Microsystems and Instrumentation Laboratories (LMI), Faculty of Technology Sciences, Mentouri Brothers University of Constantine 1, Constantine, Algeria*
[c] *Laboratory of Study of Electronic Materials for Medical Applications (LEMEAMED), Mentouri Brothers University of Constantine 1, Constantine, Algeria*
[d] *Abd elHafid Boussouf University Center of Mila, Mila, Algeria*
[e] *Faculty of science and technology, El bachir El Ibrahimi University of Borj Bou-Arreridj, Borj Bou-Arreridj, Algeria*
[f] *Renewable Energy Development Center (CDER), Algiers, Algeria*

In this work, we reconstructed the refractive index from transmission spectra obtained by the ultraviolet-visible characterization technique of Zinc Oxide thin films deposited by electrodeposition technique at an electric current density of 28.86 mA/cm² and then a high temperature treated at 450°C for 1.5 h in air. After, the results obtained are applied in GaAs PIN Photodiode to improve the spectral response of this device. The ZnO thin films with reconstructed optical properties increase and decrease respectively the transmission and reflection coefficients of GaAs PIN Photodiode; this produced an enhancement of device the spectral response.

(Received February 26, 2025; Accepted May 14, 2025)

Keywords: Reconstructed, Refractive index, ZnO, GaAs PIN photodiode

1. Introduction

In recent years, Zinc Oxide thin films have drawn notice because of their superior optical and electrical capabilities. ZnO is an II-VI semiconducting material belonging to the family of transparent metal oxides. ZnO exhibits unique optical properties in the optoelectronic field, allowing it to function in photovoltaic applications [1]. Although ZnO thin films have several uses in a variety of fields including thin film gas sensors [2,3], photodiode devices [4], piezoelectric devices [5], solar cells [6-12], biomedicine [13], etc. The optoelectronics device based on thin solid film structure with different complex refractive index $n^*=n-ik$ (where k is the extinction index and n refractive index) are interesting, this can be produced on a substrate of definite thickness d [14], by variously methods including sol-gel method [15], pulsed laser method [16], chemical vapor deposition [17], magnetron sputtering [18] and electrodeposition method [19-26]. The elaborated thin ZnO on glass by the electrodeposition technique is based on the preparation of a solution of $ZnSO_4$ in distilled water to have a concentration of 0.02M with pH = 5.0 used in an electrolysis cell, powered by a current source in order to produce a metallic layer of Zinc then anneal it at high temperature [19]. Following the deposition procedure, a nanometric Zinc film covering the slides of glass substrates, a thermal annealing at 450 °C for 90 min in air was applied to ensure complete oxidation of this layer [19]. In this paper an algorithm is proposed to allow the reconstruction of the deposited thin ZnO refractive index as a function of the wavelength λ from experimental transmission. After, the results of this algorithm's programming by means of Matlab software validated using COMSOL-Multiphysics software based on FEM (finite element method) numerical method. Finally, and for studies the effect of this thin ZnO on the opto-electrical

* Corresponding author: toufik.mouet@univ-constantine3.dz
https://doi.org/10.15251/JOR.2025.213.297

response of an GaAs PIN Photodiode, the reconstructed thin ZnO refractive index is used in this device model designed in COMSOL-Multiphysics software.

2. Physico-mathematical and technical approach

As shown in Fig. 1, which presented the studied structure with ZnO thin film, where the structure is composed of three layers visible composed of three layers: Air, ZnO and Glass, where n1, n2 and n3 are the refractive index of Air, ZnO and Glass respectively, and the thickness of ZnO is d=85 (nm) [19].

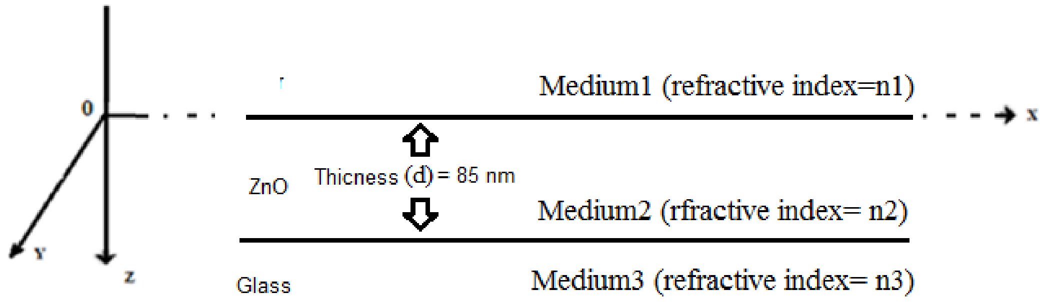

Fig. 1. Structure studied.

The transmission of the stack is then given by [27]:

$$T = \left(\frac{k_{z3}}{k\, n_1 cos(\theta_1)}\right)\left|\frac{1}{S_{22}}\right|^2 \tag{1}$$

where,
θ1: is the incidence angle,
k: the vacuum propagation vector (k=2π/λ),
λ: the wave length,
k_{z3} : The composite of propagation vector in z direction (Midium3) given by [28,29]:

$$k_{z3} = \sqrt{(k \times n_3)^2 - (k_x)^2} \tag{2}$$

k_x : The composite of propagation vector in x direction given by:

$$k_x = k_{x1} = k_{x2} = k_{x3} = k\, n_1 sin(\theta_1) \tag{3}$$

S_{22}: The one component of total matrix transfer field in the structure given by [27,30]:

$$S = \begin{pmatrix} S_{11} & S_{12} \\ S_{21} & S_{22} \end{pmatrix} = H_{12} L_2 H_{23} \tag{4}$$

where L_2 is the transaction matrix through the medium 2 using a phase factor e^{β_2} and H_{ij} is the field's matrix the transition on the interface between the medium i and j, this matrix are given by equation (5) and (6) respectively [27]:

$$\mathrm{L}_2 = \begin{pmatrix} e^{-\beta_2} & 0 \\ 0 & e^{\beta_2} \end{pmatrix} \tag{5}$$

$$\mathrm{H}_{ij} = \frac{1}{\tau_{ij}}\begin{pmatrix} 1 & \rho_{ij} \\ \rho_{ij} & 1 \end{pmatrix} \tag{6}$$

τ_{ij} and ρ_{ji} are given by [27]:

$$\tau_{ij} = \frac{2(\tilde{n}_i/\tilde{n}_j)}{1+b} \tag{7}$$

and:

$$\rho_{ji} = \frac{1-b}{1+b} \tag{8}$$

where:

$$b = \left(\frac{\tilde{n}_i}{\tilde{n}_j}\right)^2 \left(\frac{k_{z,j}}{k_{z,i}}\right) \tag{9}$$

where, $k_{z,j}$ is the reciprocal wave number of the Electrical field in the medium j, and $\tilde{n}_i$ and $\tilde{n}_j$ are the medium complex refractive index.

The β_2 coefficient is given by [27]:

$$\beta_2 = k_{z2}\mathrm{d} \tag{10}$$

k_{z2} : The composite of propagation vector in z direction (Midium2) given by:

$$k_{z2} = \sqrt{(k \times n_2)^2 - (k_x)^2} \tag{11}$$

The reconstruction of the refractive index n_{ZnO} based on Matlab software and flowchart presented in fig.2, where the n_{ZnO} initialized by the first value one (n_{ZnO}=1) and the simulated transmission calculated from theatrical model clarified in precedent, after the error between simulated and experimental transmission is calculated and if this error greater than or equal the tolerance EPS (EPS=10^{-4}), the n_{ZnO} adjusted by dn (dn=10^{-4}) and the simulated transmission recalculated. This steps is repeated until the error between simulated and experimental transmission less than the tolerance EPS (EPS=10^{-4}). In second step and for validate the result of n_{ZnO} reconstructed, the simulation of transmission based on n_{ZnO} reconstructed in the structure studied is realized in COMSOL software.

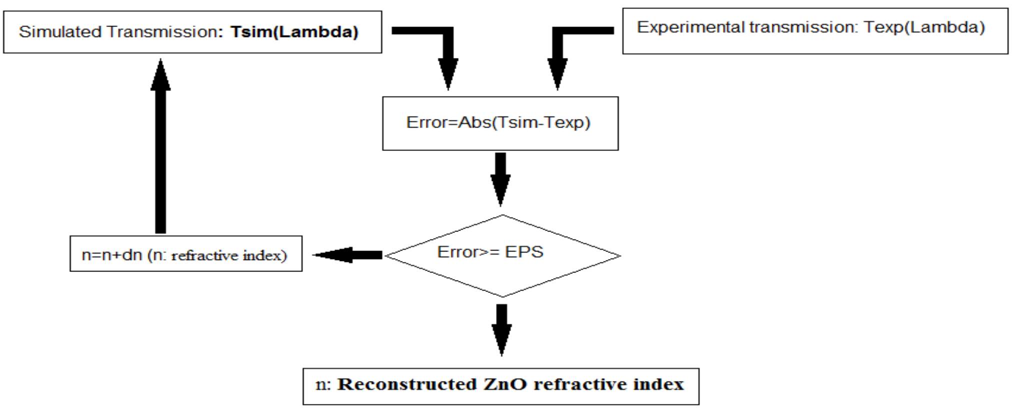

Fig. 2. Flowchart of the refractive index reconstruction technique.

Finally, the thin ZnO with the optical proprieties reconstructed is integrated in above of GaAs PIN Photodiode to ameliorate the opto-electrical response of this device.

3. Results and discussion

The reconstruction of refractive index n_{ZnO} of thin ZnO presented in fig.1 based on experimental transmission [19] is shown in Fig. 3.a. The obtained refractive index profile of thin ZnO is represented in Fig. 4. We notice that n_{ZnO} confined between 2.89 and 1.51 in visible wavelength. We notice also that reconstructed transmission profile based on n_{ZnO} is superposed to experimental transmission (Fig. 3.b)

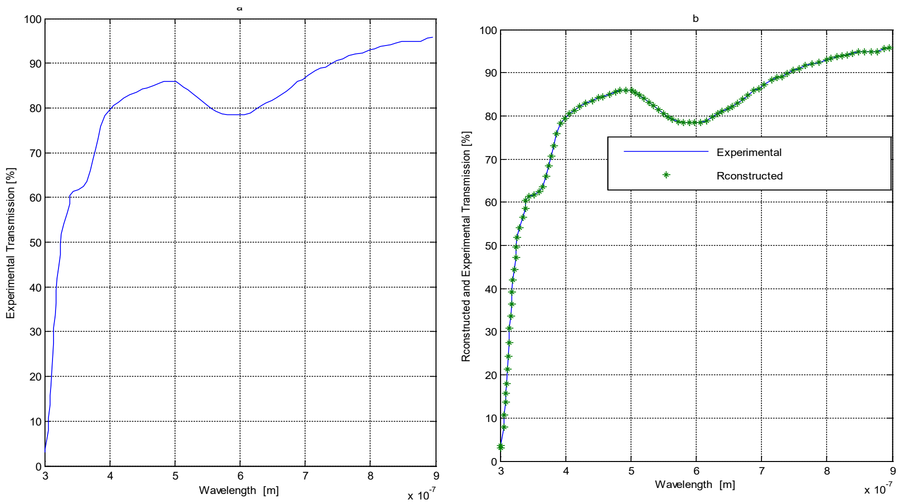

Fig. 3. a) Transmission spectra obtained by the ultraviolet-visible characterization technique of ZnO thin films deposited by electrodeposition at a current density of 28.86 mA/cm² and a thermal annealing at 450°C applied for 1.5 h in air [19]. b) Reconstructed transmission.

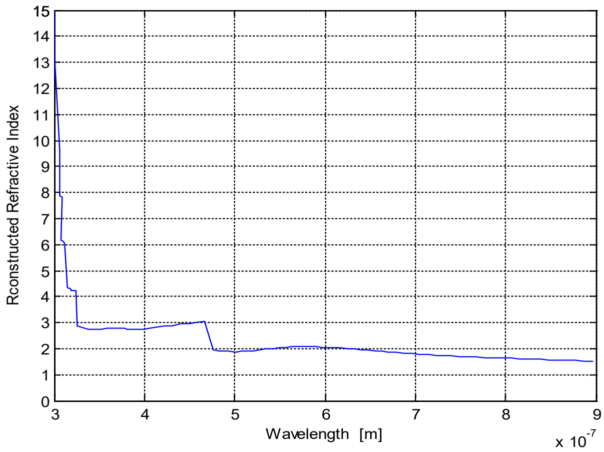

Fig. 4. Reconstructed ZnO refractive index.

In the goal to validate the results of n_{ZnO} reconstructed, we realized the simulation of transmission coefficient based on same structure studied (Fig. 1) by COMSOL-Multiphysics software, the structure dimension and mesh profile is presented in fig. 5, we notice that ZnO thickness and Glass refractive index equal to 85 (nm) and 1.51 respectively. The problem is resolved by finite element method (FEM) integrated in software, the transmission coefficient result is presented in fig.6. The fig.7 present comparison between experimental transmission coefficient (Fig. 3a) and software simulation profile (Fig. 6), we notice that two profiles are superposed which entails credibility of n_{ZnO} reconstruction results.

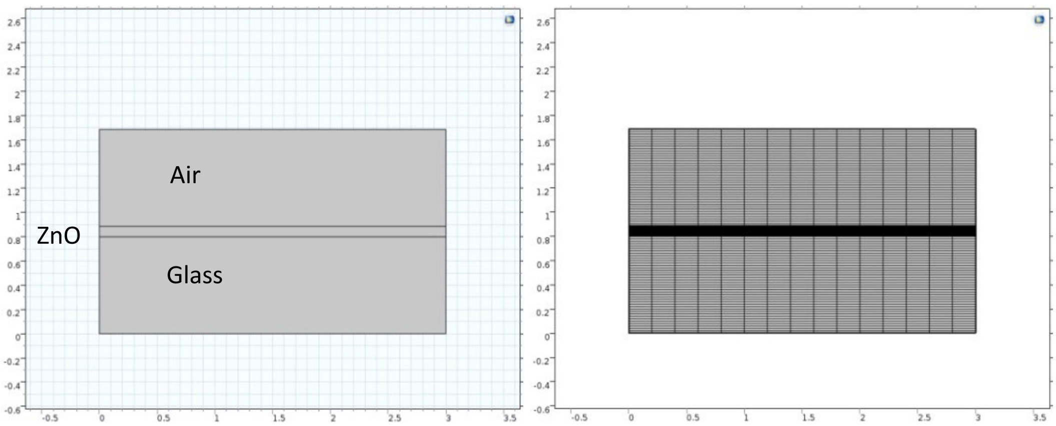

Fig. 5.a) the structure studied (dimension in µm), b) Mesh.

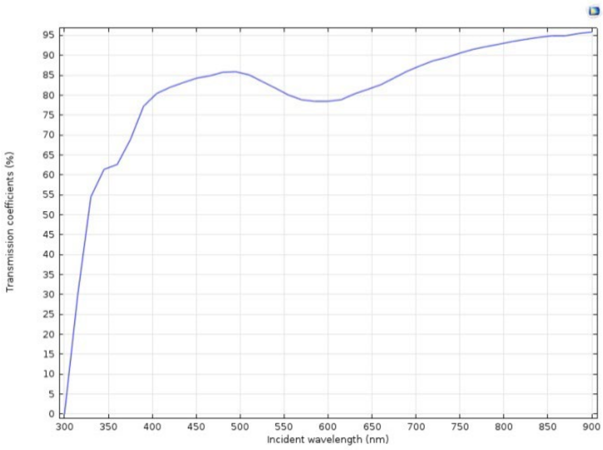

Fig. 6. Comsol simulation of transmission coefficients of structure studied as a function of the incident wavelength.

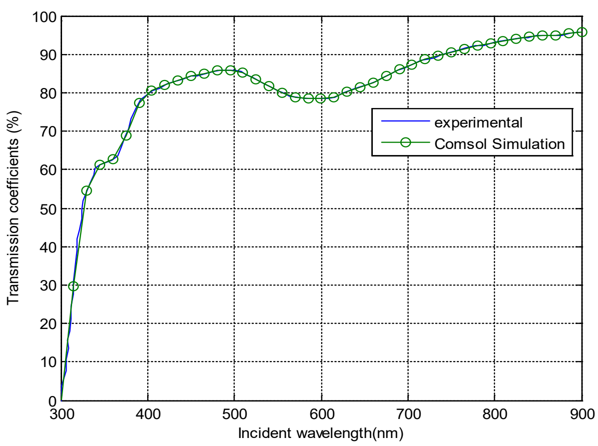

Fig. 7. Convergence between the experimental transmittance spectra and that of the Comsol simulation of the structure studied.

The model of GaAs PIN structure with layer of ZnO is studied by COMSOL-Multiphysics software. The geometry and mesh profile are shown in Fig .8. The dopant profile in the PIN structure is shown in (Fig. 9), where thin heavily doped n and p type layers adjacent to the bottom and top surfaces, respectively, are clearly visible. A large intrinsic (undoped) region of about 0.6 μm appears between the thin heavily doped layers of the surfaces. The p-type doping shows negative values while the n-type doping shows positive values. The choice of this device with the geometric and physical parameters is for the purpose of studying the effect of thin ZnO on the optoelectric response.

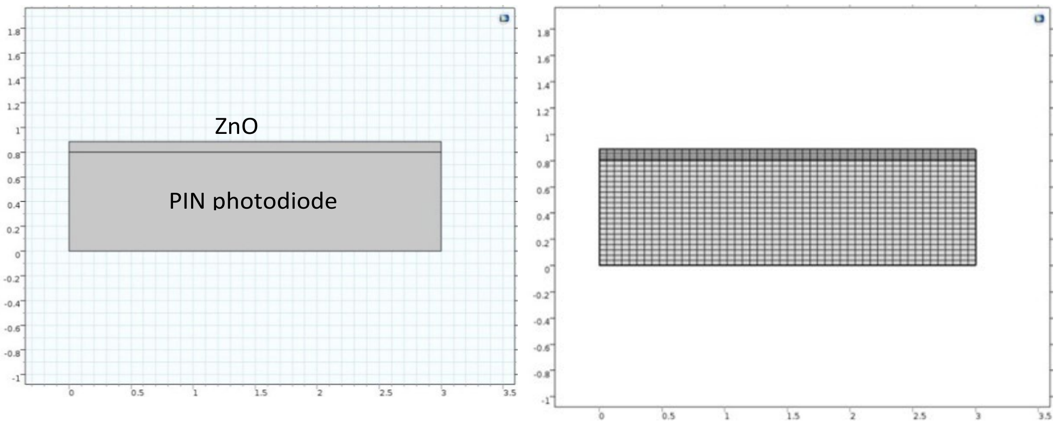

(a) *(b)*

Fig. 8.a) GaAs PIN Photodiode with ZnO thin film (dimension in μm), b) Mesh.

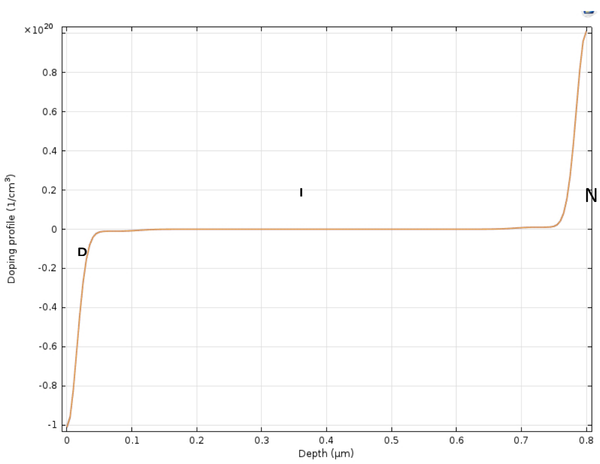

Fig. 9. Doping profile of GaAs PIN photodiode.

In the following results, the PIN device is conditioned by: reverse polarization with V_{PN}=2 (V), Pin= 10 (w) incident power of wave plane in TE mode with φ=0 (rad) angle of incident.

The transmission coefficient of GaAs PIN Photodiode versus of the incident wavelength curve is presented in fig.10. The fig.11 showing a comparison between transmission coefficient without thin ZnO (Air) (Fig. 10.a) and second with thin ZnO (Fig. 10.b), we notice that thin ZnO increase the transmission by 15 (%) to 20 (%).

The reflection spectra of GaAs PIN Photodiode are presented in fig.12. In fig.13 shown the comparison between reflection coefficient without thin ZnO (Air) (Fig. 12.a) and second with thin ZnO (Fig. 12.b), we notice that thin ZnO decrease the reflection by 15 (%) to 20 (%).

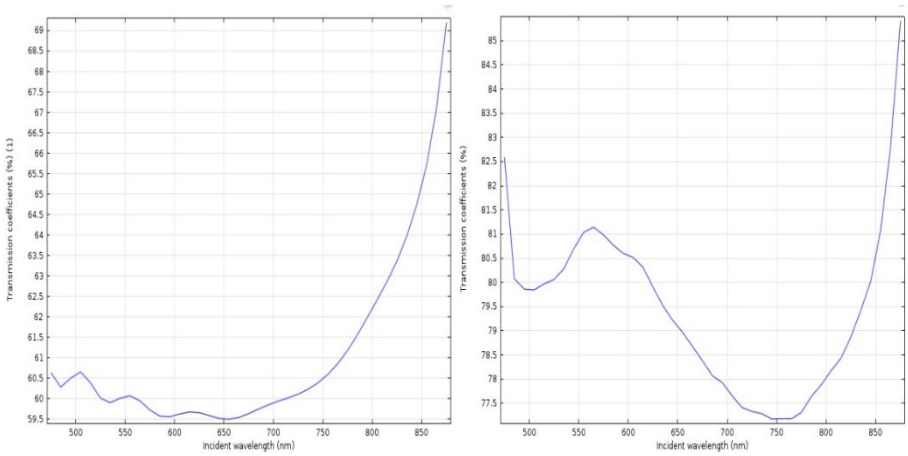

(a) *(b)*

Fig. 10. Calculated Transmission spectra of Gallium Arsenide (GaAs) PIN Photodiode: a) Air, b) ZnO.

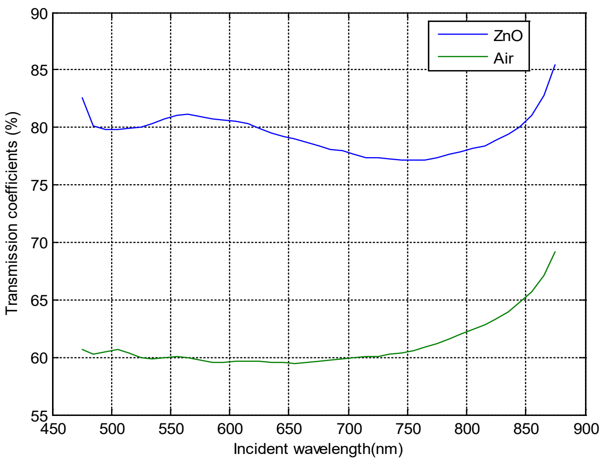

Fig. 11. Transmission coefficients of GaAs PIN Photodiode (Air and ZnO) as a function of the incident wavelength.

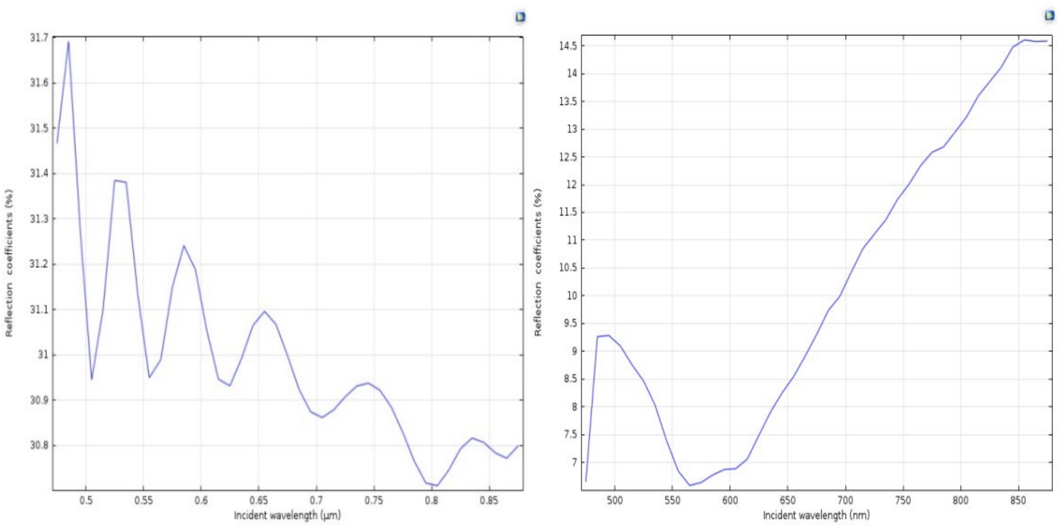

(a) *(b)*

Fig. 12. Comparison between the simulations of the Reflection spectra for the proposed PIN Photodiode structure with: a) Air and b) ZnO.

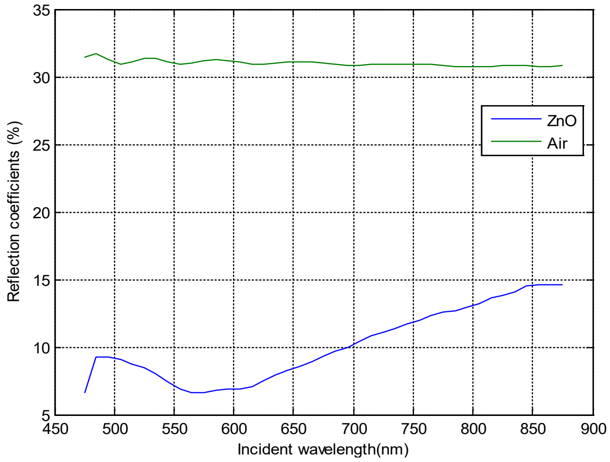

Fig. 13. Reflection coefficients of GaAs PIN Photodiode (Air and ZnO) as a function of the incident wavelength.

Figure 14 shown the electrical current generated in the studied device versus of the wavelength of the incident photon. The GaAs material having a bandgap of 1.424 (eV), where relates to a wavelength of about 872 (nm). However, the energy of the incident photon extends from below the band gap to the middle of the visible spectrum in blue region. At the long-wave end of the scale, the current flux drops to zero ; this is consisted because the energy of the longest wavelengths should not be absorbed since it is below the bandgap. In Figure 14.a showed the device without ZnO layer (air), where the current surprisingly rises to a peak rate of ~0.52 (µA) at 720 nm as the wavelength drops and the photon energy increases, on the other hand in figure 14.b with the ZnO layer the peak rate becomes to ~0.67 µA, and then gradually decreases again as the photon energy increases.

The fig.15 present comparison between current without thin ZnO (Air) (Fig. 14.a) and second with thin ZnO (Fig. 14.b), we notice that thin ZnO increase the current by 0.05 (µA) to 0.15 (µA).

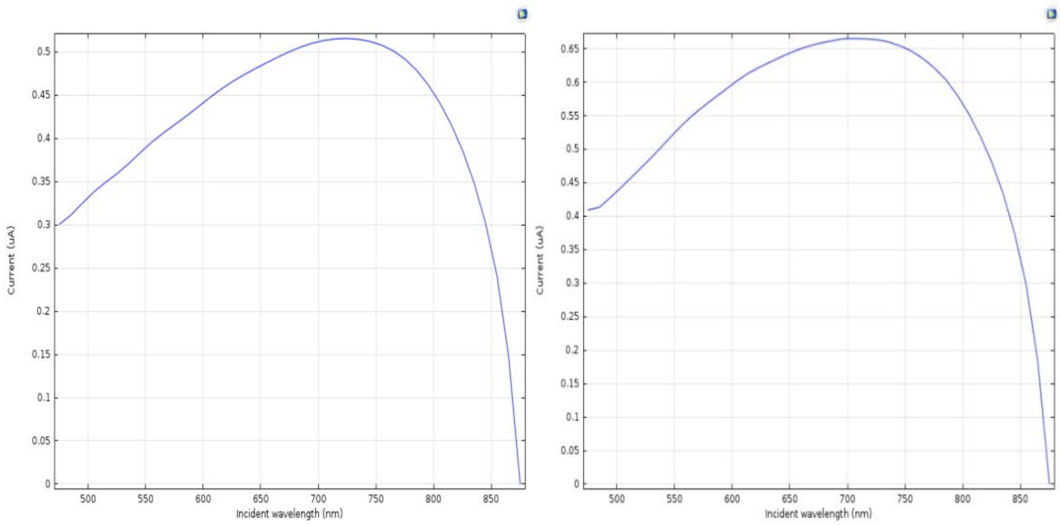

(a) *(b)*

Fig. 14. Calculated the Current output of the Photodiode component versus of the incident wavelength: a) Air, b) ZnO.

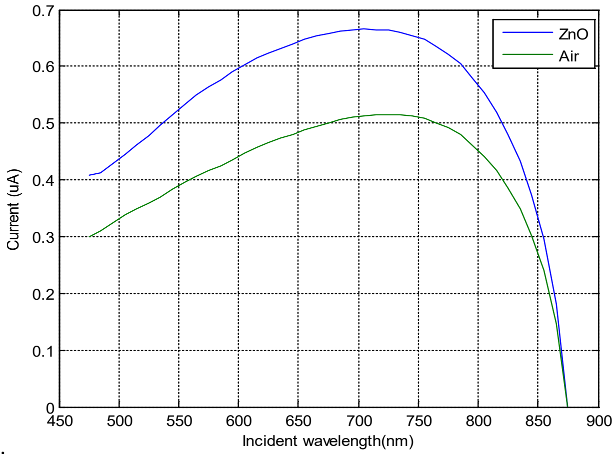

Fig. 15. Numerical simulation of Current output of GaAs PIN Photodiode with (Air and ZnO) versus of the incident wavelength.

4. Conclusion

In this work, we have carried out the reconstruction of the refracted index from the transmission spectra attained by the UV-visible technique of ZnO thin films formed by electrodeposition at an electric current density of 28.86 mA/cm² and then annealed at 450°C for 1.5 h in air. The obtained refracted index profile is used in simulation of transmission spectra of the same structure by finite element method integrated in COMSOL-Multiphysics software; the transmission coefficient result is superposed to the experimental transmission coefficient, what validates the reconstruction results. After, to prove the amelioration of the ZnO thin films on GaAs PIN Photodiode performance, a simulation of the response of this device with and without thin ZnO layer was performed by COMSOL-Multiphysics software; the obtained results show that this layer increase and decrease the transmission and reflection coefficient respectively by 15 (%) to 20 (%) of the studied device, what results an augmentation in current device response by 0.05 (µA) to 0.15 (µA).

References

[1] H. el Marouazi, A. el Hichou, Journal of Optoelectronics and Advanced Materials **25**(5-6), 289 (2023).

[2] S. Pati, P. Banerji, S.B. Majumder, Rsc Adv, 5, 6123(2015); https://doi.org/10.1039/C5RA10919A

[3] I. Y. Y. Bu, C. C. Yang, Superlattices and Microstructures 51(6), 745(2012); https://doi.org/10.1016/j.spmi.2012.03.009

[4] N. Park, K. Sun, Z. Sun, et al, J Mater Chem C, 1(44), 7333(2013); https://doi.org/10.1039/c3tc31444h

[5] Z.L. Wang, J. Song, Science. 312(5771), 242(2006); https://doi.org/10.1126/science.1124005

[6] K.S. Leschkies, T.J. Beatty, M.S. Kang, ACS Nano, 3(11), 3638(2009); https://doi.org/10.1021/nn901139d

[7] K.S. Shin, H.J. Park, B. Kumar, et al, J Mater Chem, 21(33),12274 (2011); https://doi.org/10.1039/c1jm10914f

[8] S. H. Jeong, B. N. Park, D. G. Yoo, J. H. Boo, J Korean Phys Soc, 50(3), 622(2007); https://doi.org/10.3938/jkps.50.622

[9] A. V. Balan, P. Gopinath, V. Radhika, Journal of Ovonic Research, 20(1), 85 (2024) ; https://doi.org/10.15251/JOR.2024.201.85

[10] P. Sreedev, V. Rakhesh, , Journal of Ovonic Research, 20(4), 551 (2024) ; https://doi.org/10.15251/JOR.2024.204.551

[11] M. Vetrivel, A. Jagadeeshwaran, B. Sangeetha, Journal of Ovonic Research 20(6), 841 (2024). https://doi.org/10.15251/JOR.2024.206.841

[12] N. Annab, T. Baghdadli, S. Mamoun, A. E. Merad, Journal of Ovonic Research 19 (4), 421 (2023). https://doi.org/10.15251/JOR.2023.194.421

[13] S. Singh, P. Chakrabarti, Superlattices and Microstructures, 64, 283(2013); https://doi.org/10.1016/j.spmi.2013.09.031

[14] H. Hehl, K., W. Wesch, Physica Status Solidi (A), 58(1), 181(1980); https://doi.org/10.1002/pssa.2210580122

[15] A.A.G. Farrag, M.R. Balboul, J Sol-Gel Sci Technol, 82, 269(2017); https://doi.org/10.1007/s10971-016-4277-8

[16] H. Agura, A. Suzuki, T. Matsushita, et al, Thin Solid Films. 445, 263(2003); https://doi.org/10.1016/S0040-6090(03)01158-1

[17] P.H. Lei, C.H. Cheng, Mater Sci Semicond Process, 57, 220(2017); https://doi.org/10.1088/1757-899X/1053/1/012023

[18] W. Gao, Z. Li, Ceram Int, 30(7), 1155(2004); https://doi.org/10.1016/j.ceramint.2003.12.197

[19] T. Mouet, T. Devers, A. Telia, Z. Messai, V. Harel, K. Konstantinov, et al., Applied Surface Science, 256(13), 4114 (2010); https://doi.org/10.1016/j.apsusc.2010.01.093

[20] D. Lincot, Thin Solid Films. 487(12), 40(2005); https://doi.org/10.1016/j.tsf.2005.01.032

[21] T. Mahalingham, V.S. John, M. Raja, Y.K. Su, P.J. Sebastian, Sol. Cells, 88(2), 227(2005); https://doi.org/10.1016/j.solmat.2004.06.021

[22] J.S. Wellings, N.B. Chaure, S.N. Heavens, I.M. Dharmadasa,Thin Solid Films, 516(12) 3893(2008); https://doi.org/10.1016/j.tsf.2007.07.156

[23] B.N. Illy, A.C. Cruickshank, S. Schumann, R. Da Campo,T.S. Jones, S. Heutz, et al, J Mater Chem, 21(34), 12949(2011); https://doi.org/10.1039/c1jm11225b

[24] Z. Messai, T. Devers, T. Mouet, Z. Ouennoughi, A. Boussahoul, A. Gamoura , Alexandria Engineering Journal, 57(4), 3671(2018); https://doi.org/10.1016/j.aej.2018.01.017

[25] Z. Messaï, Z. Ouennoughi, T. Devers, T. Mouet, V. Harel, K. Konstantinov, N. Bouguechal, Applied Surface Science, 257(2), 216(2010); https://doi.org/10.1016/j.apsusc.2010.07.045

[26] A. Ait hssi, A. Soussi, R. Haounati, A. Elfanaoui, A. Ihlal, K. Bouabid, Optical Materials, 160(39), 116748(2025); https://doi.org/10.1016/j.optmat.2025.116748

[27] Thomas E, Furtak Miles V Klein, Optics wely, 2eme edition (1986).

[28] J. Singh, Optical properties of condensed matter and applications. John Wiley, Chichester, England; Hoboken, NJ, 434 (2006).

[29] A. Saouli, C. Saouli, U.P.B. Sci. Bull., Series C: Electrical Engineering and Computer 83 (2), 209 (2021).

[30] B. Aliche, A. Saouli, Digest Journal of Nanomaterials and Biostructures, 19(2),731 (2024); https://doi.org/10.15251/DJNB.2024.192.731